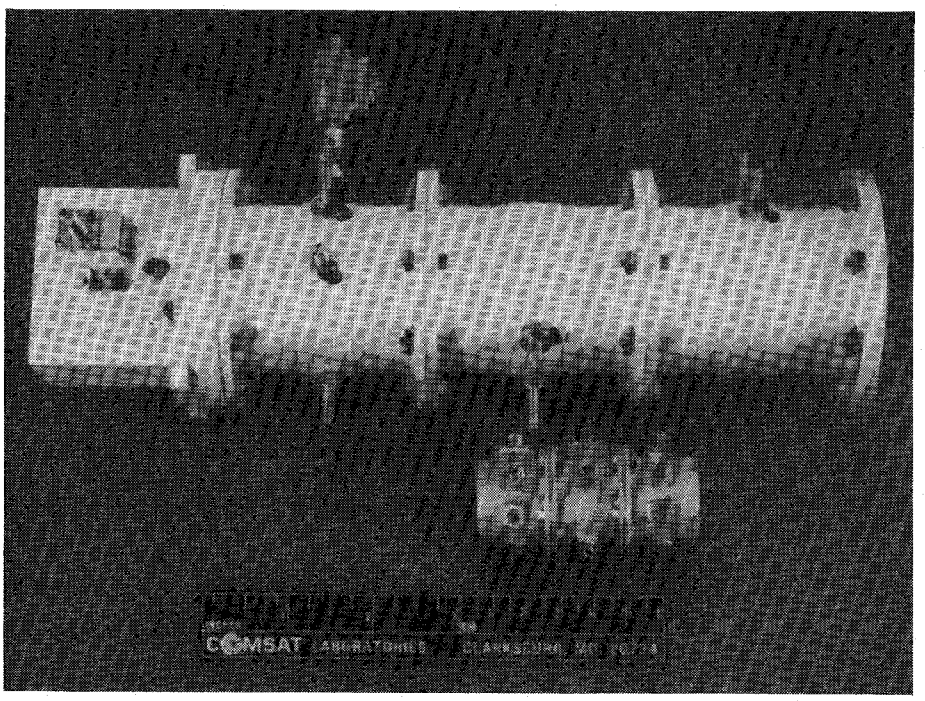

Fig. 11. Comparison of the *C*-band dual-mode dielectric-function filter and a *C*-band air-filled dual-mode filter.

References

[1] S. Darlington, "Synthesis of reactance—Four poles which produce prescribed insertion loss characteristics," *J. Math. Phys.*, vol. 18, Sept. 1939.

[2] R. M. Livingston, "Predistorted waveguide filters," *G-MTT Int. Microwave Symp., Dig.*, 1969, pp. 291–297.

[3] M. H. Chen and C. E. Mahle, "Design of a lossy waveguide filter," *COMSAT Tech. Rev.*, vol. 5, no. 2, pp. 387–398, 1975.

[4] A. E. Atia, A. E. Williams, and R. W. Newcomb, "Narrowband multiplexer-coupled cavity synthesis," *IEEE Trans. Circuits Sys.*, vol. CAS-21, pp. 649–655, Sept. 1974.

Singularity Extraction from the Electric Green's Function for a Spherical Resonator

M. BRESSAN AND G. CONCIAURO

Abstract—**The electric dyadic Green's function for a spherical resonator is expressed as a sum of two dyadics given in closed form and a dyadic given in the form of a series. The first two dyadics diverge at the source point and they represent a low-frequency approximation for the Green's function, valid up to frequencies moderately lower than the resonant frequency of the dominant mode. The dyadic given in the form of a series is finite at the source and takes into account cavity resonances. It is given either as a one-index series, whose terms are transcendental functions of the frequency, or as a double series, whose terms are rational functions of the frequency. Both series have very good converging properties everywhere inside the cavity.**

I. Introduction

The electric field at any point inside a cavity resonator bounded by a perfectly conducting wall, filled with a linear, isotropic, homogeneous medium with constitutive parameters ϵ, μ, and excited by time-harmonic ($\exp j\omega t$) electric sources may be expressed as

$$\boldsymbol{E}(\boldsymbol{r}) = -j\omega\mu \lim_{\delta \to 0} \int_{V - V_\delta} \overline{\boldsymbol{G}}_e(\boldsymbol{r}, \boldsymbol{r}', k) \cdot \boldsymbol{J}(\boldsymbol{r}')\, dv' - \frac{\overline{\boldsymbol{L}} \cdot \boldsymbol{J}(\boldsymbol{r})}{j\omega\epsilon}. \tag{1}$$

In this expression, $\boldsymbol{r}, \boldsymbol{r}'$ are the observation and the source points, respectively, $k = \omega\sqrt{\epsilon\mu}$, $\boldsymbol{J}$ is the current density, $\overline{\boldsymbol{G}}_e$ is the dyadic Green's function of the electric type, V is the cavity volume, V_δ is a principal volume about $\boldsymbol{r}$ having dimensions proportional to δ, and, finally, $\overline{\boldsymbol{L}}$ is a constant dyadic which is determined only from the geometry of V_δ [1]. Numerical calculations of $\boldsymbol{E}$ may be performed conveniently using a generalization of (1), differing from it for V_δ being allowed to be finite and for the inclusion of a further integral over V_δ, involving $\overline{\boldsymbol{G}}_e$ [2].

Green's functions for bounded regions are usually given in the form of modal expansions, obtained by general procedures such as those described by Tai [3] and Felsen–Marcuvitz [4]. Examples of these expansions are given in [5]–[8] and in the next section. Though being of great theoretical interest, such modal series are unsuitable for use in numerical algorithms (moment method, for instance) which require the computation of the electric field inside the source region. In this case, indeed, the Green's function must be computed at points $\boldsymbol{r}'$ close to $\boldsymbol{r}$, where the convergence of the series is very poor due to the singularity of $\overline{\boldsymbol{G}}_e$ at $\boldsymbol{r}' = \boldsymbol{r}$. We recall that, in three-dimensional Green's functions, this singularity is of the order R^{-3}, where R is the distance between the source and the observation points.

This drawback can be avoided by using expressions where a diverging term, expressed in closed form, is extracted from the modal expansion of $\overline{\boldsymbol{G}}_e$, so that the remaining series represents a function finite at $\boldsymbol{r}' = \boldsymbol{r}$. This series, in fact, is expected to converge very well everywhere. In this paper, we deduce an expression of this type for a spherical resonator.

Manuscript received March 7, 1984; revised January 4, 1985.

The authors are with the Dipartimento di Elettronica dell'Università di Pavia, Strada Nuova 106/c, 27100 Pavia, Italy.

0018-9480/85/0500-0407$01.00 ©1985 IEEE

In their general discussion on Green's function for closed regions, Howard and Seidel [9] considered the extraction of a singular irrotational term which represents the quasi-static approximation of $\bar{G}_e$. As explained in the following, the extraction of this term permits one to enucleate the dominant singularity (R^{-3}) of the Green's function but, in spite of this, the residual series still represents a function singular like R^{-1}. For this reason, though this series converges better than the original one, its convergence is still poor when r and r' are close to each other. A numerical example in this connection will be given at the end of this paper.

In a recent work, Daniele and Orefice [10] considered a decomposition of the Green's function into two modal series, the former singular, the latter regular at the source. As discussed in a previous paper by Daniele [11], the particular form of the singular series permits one to transform (1) in such a way to avoid the problems deriving from the nonintegrability of the singularity of the Green's function. Anyway, it is pointed out that, also after this transformation, the integral expression of the electric field exhibits a kernel diverging like R^{-1}. The series representing this kernel is expected to have converging properties similar to those of the Howard–Seidel residual series.

More recently [12], [13], we considered a new form of $\bar{G}_e$ consisting of the sum of three terms

$$\bar{G}_e = \bar{G}_t + \bar{G}_s + \bar{G}_s' \tag{2}$$

where $\bar{G}_t$ represents the irrotational part of $\bar{G}_e$ and $\bar{G}_s + \bar{G}_s'$ represents its solenoidal part. Each of the three dyadics satisfies the same boundary condition fulfilled by $\bar{G}_e$, that is,

$$\boldsymbol{n} \times \bar{\boldsymbol{G}} = 0. \tag{3}$$

For three-dimensional cavity resonators bounded by a single conducting wall, the three dyadics are expressed as [13]

$$\bar{G}_t = -\frac{1}{k^2}\nabla\nabla'\left[\frac{1}{4\pi R} + g_0(\boldsymbol{r}, \boldsymbol{r}')\right] \tag{4a}$$

$$\bar{G}_s = \frac{1}{8\pi R}\left(\bar{I} + \frac{\boldsymbol{R}\boldsymbol{R}}{R^2}\right) + \bar{G}_s^0(\boldsymbol{r}, \boldsymbol{r}') \tag{4b}$$

$$\bar{G}_s' = k^2 \sum_i \frac{\boldsymbol{e}_t(\boldsymbol{r})\boldsymbol{e}_t(\boldsymbol{r}')}{k_t^2(k_t^2 - k^2)} \tag{4c}$$

where $\bar{I}$ is the unit dyadic, $\boldsymbol{R} = \boldsymbol{r} - \boldsymbol{r}'$, g_0 is a harmonic function such that $(1/4\pi R + g_0)/\epsilon$ represents the electrostatic potential generated inside the cavity by a unity point charge placed at $\boldsymbol{r}'$, $\bar{G}_s^0$ is a *k-independent* dyadic, everywhere finite and depending on the boundary (the defining equation for $\bar{G}_s^0$ is irrelevant for the following discussion and it is not reported here), and $\boldsymbol{e}_t, k_t$ are the normalized electric modal fields and the corresponding resonant wavenumbers of the cavity.

The analysis reported in [13] permits one to state that the diverging behavior of $\bar{G}_e$ at $R = 0$ is dictated only by the R-dependent terms in (4a,b). Then, the decomposition (2) is advantageous because the diverging term

$$-\frac{1}{k^2}\nabla\nabla'\frac{1}{4\pi R} + \frac{1}{8\pi R}\left(\bar{I} + \frac{\boldsymbol{R}\boldsymbol{R}}{R^2}\right)$$

is evidenced in closed form so that the remaining part of $\bar{G}_e$ is finite at $R = 0$ and, in principle, it may be represented by rapidly converging expressions.

It is noted that $\bar{G}_t$ explicitly exhibits the dominant singularity of the Green's function and coincides with the term extracted by Howard and Seidel from the modal expansion. It is evident that, by extracting only this term, the weaker singularity (R^{-1}) is still contained in the remaining part of $\bar{G}_e$, as stated above.

It is also noted that our expression, like those proposed by Howard–Seidel and by Daniele–Orefice, permits one to transform (1) into an alternative expression not requiring the evaluation of a principal value integral, namely [13]

$$\boldsymbol{E}(\boldsymbol{r}) = -\frac{1}{\epsilon}\nabla\int_V\left[\frac{1}{4\pi R} + g_0(\boldsymbol{r}, \boldsymbol{r}')\right]\rho(\boldsymbol{r}')\,dv' - j\omega\mu\int_V\left[\bar{G}_s(\boldsymbol{r}, \boldsymbol{r}') + \bar{G}_s'(\boldsymbol{r}, \boldsymbol{r}', k)\right]\cdot\boldsymbol{J}(\boldsymbol{r}')\,dv' \tag{5}$$

where $\rho = -(\nabla\cdot\boldsymbol{J})/j\omega$ represents the charge density. This expression may be recognized as the representation of the electric field based on the scalar and the vector potentials in the Coulomb gauge.

The case of a spherical resonator has been considered as an example in the general discussion contained in [13], where a method for the direct determination of g_0 and $\bar{G}_s^0$ has been outlined. In the present work, we determine explicit expressions for g_0, $\bar{G}_s^0$, and $\bar{G}_s'$ for a spherical resonator and discuss the converging properties of the expression of $\bar{G}_e$ so obtained. The procedure followed to determine $\bar{G}_s^0$ differs from that outlined in [13] because it starts from the known modal expansion of $\bar{G}_e$ and it does not require the solution of a new boundary value problem.

An interesting feature of our result is that g_0 and $\bar{G}_s^0$ are found in closed form. Furthermore, $\bar{G}_s'$ is determined either as a rapidly converging resonant-mode double-series of the type (4c), or as a more rapidly converging radially-guided-mode one-index series. Due to their fast convergence, both of these series may be truncated up to their first few terms without significant loss of accuracy. When the resonant-mode series is truncated, the obtained approximation is a rational function of k^2, a feature that may be advantageous in treating some problems, as evidenced in [14].

II. Modal Expansion of $\bar{G}_e$

By following the general procedure described in [4, secs. 2.5, 2.6, 2.7], one can obtain the Green's function of a spherical resonator of radius a (Fig. 1) in the form

$$\bar{G}_s' = \frac{1}{k^2}(\nabla\times\nabla\times\boldsymbol{r}_0)(\nabla'\times\nabla'\times\boldsymbol{r}_0')S' + (\nabla\times\boldsymbol{r}_0)(\nabla'\times\boldsymbol{r}_0')S'' \qquad (r \neq r'). \tag{6}$$

In this expression, $\boldsymbol{r}_0$ and $\boldsymbol{r}_0'$ are the unit vectors in the directions of $\boldsymbol{r}$ and $\boldsymbol{r}'$, respectively, and the functions S' and S'' are given by

$$S' = \frac{1}{4\pi}\sum_1^\infty{}_n \frac{2n+1}{n(n+1)} Y_n \sum_0^n{}_m \frac{2(n-m)!}{\epsilon_m(n+m)!} P_n^m(\cos\vartheta)\,P_n^m(\cos\vartheta')\cdot\cos[m(\varphi - \varphi')] \tag{7a}$$

$$S'' = \frac{1}{4\pi}\sum_1^\infty{}_n \frac{2n+1}{n(n+1)} Z_n \sum_0^n{}_m \frac{2(n-m)!}{\epsilon_m(n+m)!} P_n^m(\cos\vartheta)\,P_n^m(\cos\vartheta')\cdot\cos[m(\varphi - \varphi')] \tag{7b}$$

where r, ϑ, φ; r', ϑ', φ' are the spherical coordinates of $\boldsymbol{r}$ and $\boldsymbol{r}'$, P_n^m are the associate Legendre functions, $\epsilon_m = 2$ for $m = 0$, $\epsilon_m = 1$ for $m \neq 0$. Functions $Y_n = Y_n(r, r', k)$ and $Z_n = Z_n(r, r', k)$ are the solutions of the equation

$$\left[\frac{\partial^2}{\partial r^2} + k^2 - \frac{n(n+1)}{r^2}\right]\begin{Bmatrix} Y_n \\ Z_n \end{Bmatrix} = \delta(r - r') \tag{8}$$

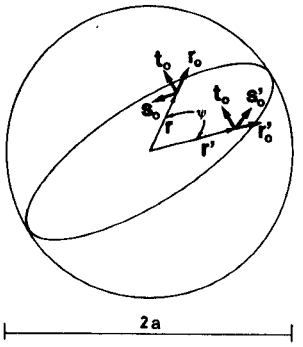

Fig. 1. The sphere and the unit vectors at the observation and the source points.

subject to the following boundary conditions:

$$Y_n, Z_n \text{ finite at } r=0; \qquad \frac{\partial}{\partial r} Y_n = 0, Z_n = 0 \text{ at } r=a. \quad (9)$$

Functions Y_n and Z_n may be determined either in closed form or as eigenfunction expansions. The closed-form solution has different definitions in the intervals $(0, r')$ and (r', a). For $0 < r < r'$, we obtain

$$Y_n = \frac{j_n(kr)}{kj_n'(ka)}\left[n_n'(ka)\, j_n(kr') - n_n(kr')\, j_n'(ka)\right] \quad (10a)$$

$$Z_n = \frac{j_n(kr)}{kj_n(ka)}\left[n_n(ka)\, j_n(kr') - n_n(kr')\, j_n(ka)\right] \quad (10b)$$

where j_n and n_n are the spherical Bessel functions, defined as

$$j_n(x) = \sqrt{\frac{\pi x}{2}}\, J_{n+1/2}(x) \qquad n_n(x) = \sqrt{\frac{\pi x}{2}}\, N_{n+1/2}(x)$$

and j_n', n_n' are their derivatives. For $r' < r < a$, the expressions for Y_n and Z_n are deduced from (10) by interchanging r and r'. The solution in the form of eigenfunctions expansion has a unique expression in the whole interval $(0, a)$, given by

$$Y_n = \sum_{1}^{\infty}{}_p \frac{2x_{np}'^2}{a\left[x_{np}'^2 - n(n+1)\right]\left(k_{np}'^2 - k^2\right)} \frac{j_n'\left(k_{np}' r\right) j_n\left(k_{np}' r'\right)}{j_n^2\left(x_{np}'\right)} \quad (11a)$$

$$Z_n = \sum_{1}^{\infty}{}_p \frac{2}{a\left(k_{np}^2 - k^2\right)} \frac{j_n\left(k_{np} r\right) j_n\left(k_{np} r'\right)}{j_{n-1}^2\left(x_{np}\right)} \quad (11b)$$

where x_{np} and x_{np}' are the zeros of j_n and j_n', and

$$k_{np} = x_{np}/a \qquad k_{np}' = x_{np}'/a$$

are the resonant wavenumbers of the TE and TM resonant modes, respectively.

It is noted that, for any value of the index n, the different values of m denote n degenerate modes; their total contribution may be taken into account by substituting the finite summation in (7) with a single term, as permitted by the well-known "addition formula" for the associate Legendre functions. It is thus obtained

$$S' = \frac{1}{4\pi} \sum_{1}^{\infty}{}_n \frac{2n+1}{n(n+1)} Y_n P_n(u) \quad (12a)$$

$$S'' = \frac{1}{4\pi} \sum_{1}^{\infty}{}_n \frac{2n+1}{n(n+1)} Z_n P_n(u) \quad (12b)$$

where $u = \cos\psi$ (see Fig. 1) and P_n functions are Legendre polynomials.

The explicit expression of $\bar{\bar{G}}_e$ in the form of a modal expansion may be obtained by applying term-wise the dyadic differential operators appearing in (6) to the series representing S' and S''. Depending on the use of (10) or (11), two types of expansions are obtained: in the form of a one-index series (radially-guided-mode expansion) or of a double series (resonant-mode expansion). Convergence properties of both series are poor. In fact, numerical calculations reveal that they converge slowly for $\boldsymbol{r}$ close to $\boldsymbol{r}'$. As an example, when $a = 1, r = 0.49, r' = 0.5, \psi = 30°$, convergence of the one-index series is observed only after having added about one thousand terms, whereas the same number of terms is not sufficient to observe convergence in the case of the double series. It is worth noting that when $\boldsymbol{r}$ is not close to $\boldsymbol{r}'$, the one-index series converges fairly well, whereas the convergence of the double series remains slow.

III. Determination of g_0

The electrostatic potential generated inside a spherical cavity by a unit charge placed at $\boldsymbol{r}'$ is easily determined by image theory and is given by

$$\frac{1}{4\pi\epsilon}\left(\frac{1}{R} - \frac{a}{r' R_i}\right) \quad (13)$$

where $R_i = [r^2 + (a^2/r')^2 - 2r(a^2/r')u]^{1/2}$ represents the distance between $\boldsymbol{r}$ and the image of the source point. Then, comparing (13) with the argument of $\nabla\nabla'$ in (4a), g_0 is immediately identified as

$$g_0 = -\frac{a}{4\pi r' R_i} = -\frac{1}{4\pi a}\left[1 - 2hu + h^2\right]^{-1/2} \quad (14)$$

where

$$h = \frac{rr'}{a^2}.$$

IV. Determination of $\bar{\bar{G}}_s^0$ in Form of a Series

From (2), (4a), (4b), and (4c), we deduce

$$\frac{1}{8\pi R}\left(\bar{\bar{I}} + \frac{\boldsymbol{RR}}{R^2}\right) + \bar{\bar{G}}_s^0(\boldsymbol{r}, \boldsymbol{r}') = \lim_{k \to 0} \frac{1}{2} \frac{\partial^2}{\partial k^2}\left(k^2 \bar{\bar{G}}_e\right). \quad (15)$$

On substitution of (6) and (12), we have

$$\begin{aligned}\frac{1}{8\pi R}\left(\bar{\bar{I}} + \frac{\boldsymbol{RR}}{R^2}\right) + \bar{\bar{G}}_s^0 = {} & (\nabla \times \nabla \times \boldsymbol{r}_0)\left(\nabla' \times \nabla' \times \boldsymbol{r}_0'\right) \frac{1}{8\pi} \\ & \cdot \sum_{1}^{\infty}{}_n \frac{2n+1}{n(n+1)} P_n(u) \frac{\partial^2}{\partial k^2} Y_n(r, r', 0) \\ & + (\nabla \times \boldsymbol{r}_0)\left(\nabla' \times \boldsymbol{r}_0'\right) \frac{1}{4\pi} \\ & \cdot \sum_{1}^{\infty}{}_n \frac{2n+1}{n(n+1)} P_n(u)\, Z_n(r, r', 0).\end{aligned} \quad (16)$$

From (10), we deduce

$$\begin{aligned}\frac{\partial^2}{\partial k^2} Y_n(r, r', 0) = {} & \frac{r}{2n+1}\left(\frac{r}{r'}\right)^n \left[\frac{r'^2}{2n-1} - \frac{r^2}{2n+3}\right] \\ & + \frac{2a^3 h^{n+1}}{(n+1)(2n+1)}\left[\frac{2n^3 + 3n^2 - 5n - 3}{(2n+3)(2n-1)(n+1)}\right. \\ & \left. - \frac{n(r^2 + r'^2)}{2(2n+3)a^2}\right]\end{aligned} \quad (17a)$$

$$Z_n(r, r', 0) = \frac{r}{2n+1}\left(\frac{r}{r'}\right)^n - \frac{a}{2n+1} h^{n+1} \quad (17b)$$

valid for $0 < r < r'$. For $r' < r < a$, similar equations hold, with r and r' interchanged on the right-hand side.

As stated in the Introduction, the dyadic (16) satisfies the boundary condition (3). Since the singular term on the left-hand side of (16) does not depend on the boundary, it follows that the regular dyadic $\bar{G}_s^0$ must depend on the radius a, in order to match the boundary condition. Moreover, due to the fact that the singular term by itself satisfies the boundary condition in the limiting case of an infinite radius, it is clear that $\bar{G}_s^0$ must go to zero when a goes to infinity. On the other hand, the series obtained on substitution of (17a,b) into the right-hand side of (16) may be split into the sum of two series, the former independent of a, the latter going to zero when a diverges. The considerations above permit one to associate $\bar{G}_s^0$ with these last series, that is to say,

$$\bar{G}_s^0 = \frac{a^3}{4\pi}(\nabla\times\nabla\times\boldsymbol{r}_0)(\nabla'\times\nabla'\times\boldsymbol{r}_0') \cdot \sum_1^n{}_n \frac{P_n(u)h^{n+1}}{(2n+3)(n+1)^2}\left[\frac{2n^3+3n^2-5n-3}{n(n+1)(2n-1)} - \frac{r^2+r'^2}{2a^2}\right] - \frac{a}{4\pi}(\nabla\times\boldsymbol{r}_0)(\nabla'\times\boldsymbol{r}_0')\sum_1^\infty{}_n \frac{P_n(u)h^{n+1}}{n(n+1)}. \quad (18)$$

It is noted that this expression has been derived from (17) valid for $0 < r < r'$. The expression for $r' < r < a$ should be obtained by interchanging r and r'. However, this interchange does not modify the series in (18) so that this expression holds everywhere.

V. Determination of $\bar{G}_s'$

From (2), (4a), (4b), and (4c), we find

$$\bar{G}_s' = \bar{G}_e - \frac{1}{k^2}\lim_{k\to 0}\left(k^2\bar{G}_e\right) - \lim_{k\to 0}\frac{1}{2}\frac{\partial^2}{\partial k^2}\left(k^2\bar{G}_e\right). \quad (19)$$

On substitution of (6) and (15), we obtain

$$\bar{G}_s' = (\nabla\times\nabla\times\boldsymbol{r}_0)(\nabla'\times\nabla'\times\boldsymbol{r}_0')\frac{1}{4\pi}\sum_1^\infty{}_n \frac{2n+1}{n(n+1)}P_n(u)U_n + (\nabla\times\boldsymbol{r}_0)(\nabla'\times\boldsymbol{r}_0')\frac{1}{4\pi}\sum_1^\infty{}_n \frac{2n+1}{n(n+1)}P_n(u)V_n \quad (20)$$

where

$$U_n = \frac{Y_n(r,r',k) - Y_n(r,r',0)}{k^2} - \frac{1}{2}\frac{\partial^2}{\partial k^2}Y_n(r,r',0) \quad (21a)$$

$$V_n = Z_n(r,r',k) - Z_n(r,r',0). \quad (21b)$$

Starting from (10), we obtain

$$U_n = \frac{j_n(kr)}{k^3}\left[\frac{n_n'(ka)\,j_n(kr')}{j_n'(ka)} - n_n(kr')\right] - \frac{r}{2(2n+1)}\left(\frac{r}{r'}\right)^n\left[\frac{2}{k^2} + \frac{r'^2}{2n-1} - \frac{r^2}{2n+3}\right] + \frac{ah^{n+1}}{(n+1)(2n+1)}\left[\frac{n(r^2+r'^2)}{2(2n+3)} - \frac{2n^3+3n^2-5n-3}{(2n-1)(2n+3)(n+1)}a^2 - \frac{n}{k^2}\right] \quad (22a)$$

$$V_n = \frac{j_n(kr)}{k}\left[\frac{n_n(ka)\,j_n(kr')}{j_n(ka)} - n_n(kr')\right] - \frac{1}{2n+1}\left[r\left(\frac{r}{r'}\right)^n - ah^{n+1}\right] \quad (22b)$$

valid for $0 < r < r'$. For $r' < r < a$, similar equations hold with r and r' interchanged.

Alternative expressions are determined starting from (11)

$$U_n = k^2\sum_1^\infty{}_p \frac{1}{k_{np}'^2\left(k_{np}'^2 - k^2\right)}\frac{2aj_n\left(k_{np}'r\right)j_n\left(k_{np}'r'\right)}{\left[x_{np}'^2 - n(n+1)\right]j_n^2\left(x_{np}'\right)} \quad (23a)$$

$$V_n = k^2\sum_1^\infty{}_p \frac{1}{k_{np}'^2\left(k_{np}'^2 - k^2\right)}\frac{2j_n\left(k_{np}r\right)j_n\left(k_{np}r'\right)}{aj_{n-1}^2\left(x_{np}\right)}. \quad (23b)$$

Using these last expressions, (20) yields $\bar{G}_s'$ in form of a resonant-mode expansion, similar to the general expression (4c).

VI. Components of $\bar{G}_e$

By symmetry considerations, it is evident that: a) a current element at $\boldsymbol{r}'$, lying on the plane of $\boldsymbol{r}$ and $\boldsymbol{r}'$, gives place at $\boldsymbol{r}$ to an electric field lying on the same plane; b) a current element at $\boldsymbol{r}'$, perpendicular to $\boldsymbol{r}$ and $\boldsymbol{r}'$, gives place at $\boldsymbol{r}$ to a field perpendicular to the same plane. For this reason, the number of components of $\bar{G}_e$ is reduced by referring the field and the source to the directions of the unit vectors $\boldsymbol{r}_0, \boldsymbol{s}_0, \boldsymbol{t}_0$ and $\boldsymbol{r}_0', \boldsymbol{s}_0', \boldsymbol{t}_0$, respectively (see Fig. 1), where

$$\boldsymbol{t}_0 = \frac{\boldsymbol{r}'\times\boldsymbol{r}}{|\boldsymbol{r}'\times\boldsymbol{r}|} \quad \boldsymbol{s}_0 = \boldsymbol{t}_0\times\boldsymbol{r}_0 \quad \boldsymbol{s}_0' = \boldsymbol{t}_0\times\boldsymbol{r}_0'. \quad (24)$$

In fact, $\bar{G}_e$ may be expressed by a form of the type

$$\bar{G}_e = \boldsymbol{r}_0\boldsymbol{r}_0'G_{rr'} + \boldsymbol{r}_0\boldsymbol{s}_0'G_{rs'} + \boldsymbol{s}_0\boldsymbol{r}_0'G_{sr'} + \boldsymbol{s}_0\boldsymbol{s}_0'G_{ss'} + \boldsymbol{t}_0\boldsymbol{t}_0G_{tt} \quad (25)$$

which requires the specification of five components only. The expressions which relate them to the nine components with respect to the fundamental unit vectors of the spherical coordinate system are reported in Appendix I.

By examining (14), (18), and (20), we see that the determination of the components of $\bar{G}_e$ requires the differentiation of functions depending only on the spatial variables r, r', and u. It may be shown that, when applied to a function of this type, the dyadic differential operators involved in the calculation of $\bar{G}_e$ may be expressed as follows:

$$\nabla\nabla' = \boldsymbol{r}_0\boldsymbol{r}_0'\frac{\partial^2}{\partial r\,\partial r'} + \boldsymbol{r}_0\boldsymbol{s}_0'\frac{v}{r'}\frac{\partial^2}{\partial r\,\partial u} - \boldsymbol{s}_0\boldsymbol{r}_0'\frac{v}{r}\frac{\partial^2}{\partial r'\,\partial u} - \frac{\boldsymbol{s}_0\boldsymbol{s}_0'}{rr'}\left(u\frac{\partial}{\partial u} + L\right) + \frac{\boldsymbol{t}_0\boldsymbol{t}_0}{rr'}\frac{\partial}{\partial u} \quad (26a)$$

$$(\nabla\times\boldsymbol{r}_0)(\nabla'\times\boldsymbol{r}_0') = \frac{\boldsymbol{s}_0\boldsymbol{s}_0'}{rr'}\frac{\partial}{\partial u} - \frac{\boldsymbol{t}_0\boldsymbol{t}_0}{rr'}\left(u\frac{\partial}{\partial u} + L\right) \quad (26b)$$

$$(\nabla\times\nabla\times\boldsymbol{r}_0)(\nabla'\times\nabla'\times\boldsymbol{r}_0') = \boldsymbol{r}_0\boldsymbol{r}_0'\frac{1}{r^2r'^2}L^2 - \boldsymbol{r}_0\boldsymbol{s}_0'\frac{v}{r^2r'}L\frac{\partial^2}{\partial r'\,\partial u} + \boldsymbol{s}_0\boldsymbol{r}_0'\frac{v}{rr'^2}L\frac{\partial^2}{\partial r\,\partial u} - \frac{\boldsymbol{s}_0\boldsymbol{s}_0'}{rr'}\left(u\frac{\partial}{\partial u} + L\right)\frac{\partial^2}{\partial r\,\partial r'} + \frac{\boldsymbol{t}_0\boldsymbol{t}_0}{rr'}\frac{\partial^3}{\partial r\,\partial r'\,\partial u} \quad (26c)$$

where

$$v = \sqrt{1-u^2} = \sin\psi \quad L = v^2\frac{\partial^2}{\partial u^2} - 2u\frac{\partial}{\partial u}.$$

It is noted that $LP_n(u) = -n(n+1)P_n(u)$.

On use of formulas (2), (26), (4a), (4b), (14), (18), and (20), $\bar{\bar{G}}_e$ is determined in the form (25). We obtain

$$G_{rr'}=\frac{1}{4\pi k^2}\left[\frac{1}{R^3}\left(2u-\frac{3rr'v^2}{R^2}\right)+\frac{1}{a^3}\cdot(h^3-h^2u+hu^2-2h+u)f_0^5\right]+\frac{1}{8\pi R}\left(2u-\frac{rr'v^2}{R^2}\right)+G^0_{rr'}+G'_{rr'} \tag{27a}$$

$$G_{rs'}=-\frac{v}{4\pi k^2}\left[\frac{1}{R^3}\left(1-3\frac{r^2-rr'u}{R^2}\right)+\frac{1}{a^3}(2h^2-hu-1)f_0^5\right]+\frac{v}{8\pi R}\left(1+\frac{r^2-rr'u}{R^2}\right)+G^0_{rs'}+G'_{rs'} \tag{27b}$$

$$G_{sr'}(r,r',u,k)=-G_{rs'}(r',r,u,k) \tag{27c}$$

$$G_{ss'}=\frac{1}{4\pi k^2}\left[\frac{1}{R^3}\left(\frac{3rr'v^2}{R^2}-u\right)+\frac{1}{a^3}(h^2u-3h+hu^2+u)f_0^5\right]+\frac{1}{8\pi R}\left(u+\frac{rr'v^2}{R^2}\right)+G^0_{ss'}+G'_{ss'} \tag{27d}$$

$$G_{tt}=-\frac{1}{4\pi k^2}\left[\frac{1}{R^3}-\frac{1}{a^3}f_0^3\right]+\frac{1}{8\pi R}+G^0_{tt}+G'_{tt} \tag{27e}$$

where f_0 is defined in (29a), and $G^0_{rr'},\cdots,G^0_{tt}$, and $G'_{rr'},\cdots,G'_{tt}$ are the components of $\bar{\bar{G}}^0_s$ and $\bar{\bar{G}}'_s$, respectively.

The series representing $G^0_{rr'},\cdots,G^0_{tt}$ (deduced from (18)) can be summed (see Appendix II). It is obtained as follows:

$$G^0_{rr'}=\frac{1}{4\pi a}\left[\left(3\frac{r^2+r'^2}{a^2}+h^2+9\right)f_1+f_2+\frac{h-3u}{4}f_0-\left(2-\frac{r^2+r'^2}{a^2}\right)\frac{h-u}{4}f_0^3\right] \tag{28a}$$

$$G^0_{rs'}=-\frac{v}{4\pi a}\left(1-\frac{r'^2}{a^2}\right)\left[\frac{3a^2+r^2}{2a^2}f_3+f_4\right]-\frac{vf_0}{16\pi a}\left[3+\frac{r^2+r'^2-2a^2}{a^2}f_0^2\right] \tag{28b}$$

$$G^0_{ss'}=\frac{1}{4\pi a}\left(1-\frac{r^2}{a^2}\right)\left(1-\frac{r'^2}{a^2}\right)\left[3f_1-uf_3-uf_4-\frac{h-u}{4}f_0^3\right]-\frac{f_0}{8\pi a}\left[u+hv^2f_0^2\right] \tag{28c}$$

$$G^0_{tt}=\frac{1}{4\pi a}\left(1-\frac{r^2}{a^2}\right)\left(1-\frac{r'^2}{a^2}\right)[f_3+f_4]-\frac{1}{8\pi a}f_0 \tag{28d}$$

where

$$f_0=(1-2hu+h^2)^{-1/2} \tag{29a}$$

$$f_1=\frac{1}{8h}\left[f_0-\frac{3}{h(1+h)}\left(\frac{F-2E}{\sin\beta}+\frac{1}{f_0}\right)\right] \tag{29b}$$

$$f_2=\frac{1}{h^2}\left[\ln\left(\frac{1/f_0+h-u}{1-u}\right)-hf_0\right] \tag{29c}$$

$$f_3=\frac{3}{4v^2h^2(1+h)}\left[(1+u)(1+h-2hu)f_0-\frac{(1-u)F+2uE}{\sin\beta}\right] \tag{29d}$$

$$f_4=\frac{1}{v^2h^2}[1+(hu-1)f_0] \tag{29e}$$

In these expressions, $F=F(\beta,K)$ and $E=E(\beta,K)$ represent the elliptic integrals of the first and second kind, respectively, of argument $\beta=\arcsin[2\sqrt{h}/(1+h)]$ and modulus $K=\sqrt{(1+u)/2}$. It is noted that, in the limiting cases where h and/or v vanish, (29b,c,d,e) are indeterminate. Anyway, an accurate analysis reveals that f_1, f_2, f_3, and f_4 remain finite and that their values for small h and/or v can be calculated using the formulas given in Appendix II.

The series representing the components of $\bar{\bar{G}}'_s$ (deduced from (20)) are

$$G'_{rr'}=\frac{1}{4\pi}\sum_1^\infty n(n+1)(2n+1)P_n(u)\frac{U_n}{r^2r'^2} \tag{30a}$$

$$G'_{rs'}=\frac{v}{4\pi}\sum_1^\infty(2n+1)P'_n(u)\frac{1}{r^2r'}\frac{\partial U_n}{\partial r'} \tag{30b}$$

$$G'_{ss'}=\frac{1}{4\pi}\sum_1^\infty(2n+1)\left[\frac{P'_n(u)V_n}{n(n+1)rr'}+\left(P_n(u)-\frac{uP'_n(u)}{n(n+1)}\right)\frac{1}{rr'}\frac{\partial^2U_n}{\partial r\,\partial r'}\right] \tag{30c}$$

$$G'_{tt}=\frac{1}{4\pi}\sum_1^\infty(2n+1)\left[\frac{P'_n(u)}{n(n+1)rr'}\frac{\partial^2U_n}{\partial r\,\partial r'}+\left(P_n(u)-\frac{uP'_n(u)}{n(n+1)}\right)\frac{V_n}{rr'}\right] \tag{30d}$$

where P'_n denotes the derivative of P_n. On substitution of (22) or (23) into (30), the components of $\bar{\bar{G}}'_s$ are obtained either in the form of a one-index series or in the form of a double series. For the sake of shortness, we omit writing down these formulas, whose derivation, however, is trivial. It is observed that the one-index series have different definitions in the intervals $(0,r')$ and (r',a), whereas the double series have a unique definition everywhere. The terms of the one-index series depend on k also through the spherical Bessel functions, whereas the terms of the double series are rational functions of k^2. As expected, the components of $\bar{\bar{G}}_e$ diverge when k approaches any of the resonating values k_{np} or k'_{np} defined above. The one-index series diverge due to the denominators $j_n(ka)$ and $j'_n(ka)$ in (22). The double series diverge due to the denominators $k^2_{np}-k^2$ and $k'^2_{np}-k^2$ in (23). When k is not coincident with a resonant wavenumber, all series converge everywhere, $\boldsymbol{r}=\boldsymbol{r}'$ included.

It is noted that if the field is evaluated using (5), the only part of $\bar{\bar{G}}_e$ involved in the calculation is $\bar{\bar{G}}_s+\bar{\bar{G}}'_s$. The components of this dyadic are recognized in the last three terms in each one of the expressions of (27).

VII. Converging Properties

The series representing the components of $\bar{\bar{G}}'_s$ are too complicated to permit a simple analysis of their converging properties. Then we base our discussion on some numerical results.

Diagrams in Fig. 2 represent successive approximations of the component $G_{rr'}$ as a function of the computing time. The first approximation (labeled with a) consists of the contribution of the term proportional to k^{-2} in (27a), i.e., the rr' component of the dyadic $\bar{\bar{G}}_t$ in (2). The second approximation (labeled with b) includes the rr' component of the dyadic $\bar{\bar{G}}_s$, i.e., it is obtained by considering all the terms in (27a), except $G'_{rr'}$. Subsequent approximations (labeled with $c,d,\cdots$) are obtained by adding each time a new term of the series representing $G'_{rr'}$ ((30a)) in the form of a one-index series (continuous line) or of double series

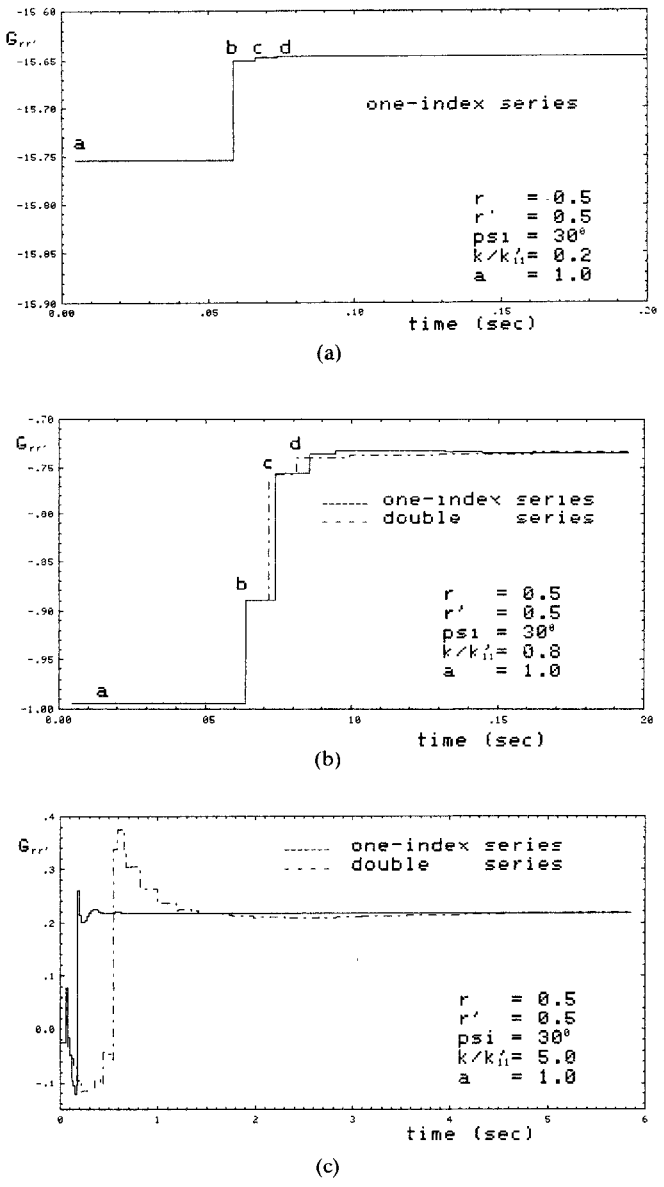

Fig. 2. Successive approximations of $G_{rr'}$ as a function of computing time, for different values of k

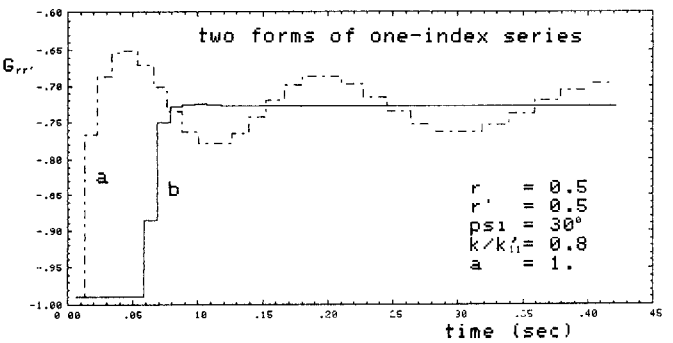

Fig. 3. Successive approximations of two expressions of $G_{rr'}$ in the form of a one-index series. Diagram a: (31). Diagram b: (2).

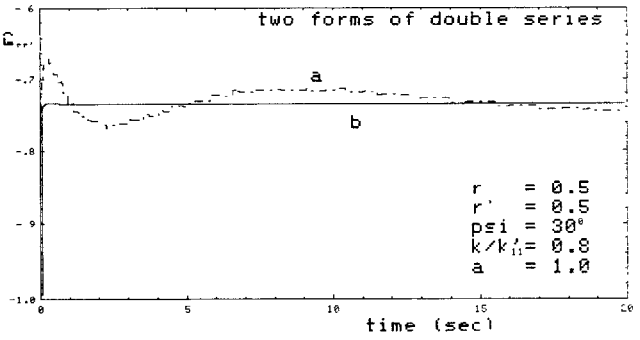

Fig. 4. Successive approximations of two expressions of $G_{rr'}$ in form of double series. Diagram a: (31). Diagram b: (2).

(dashed line). In the case of the double series, the terms are added in order of increasing resonant wavenumbers. The radius of the resonator and the positions of the observation and source points are the same in the three cases considered in Fig. 2(a), (b), and (c), whereas the values of k are different from one another.

In the case of Fig. 2(a), the frequency is moderately lower than the resonant frequency of the dominant mode ($k = k'_{11}/5$). In this diagram, the dashed line was not reported, being nearly coincident with the continuous line. It is noted that the approximation b is fairly good, i.e., the contribution of $G'_{rr'}$ may be neglected without a significant error.

In the case of Fig. 2(b), the frequency is fairly close to the frequency of the dominant mode ($k = 0.8\ k'_{11}$). Both series representing $G'_{rr'}$ converge very rapidly and the largest contribution derives from their first term, which takes into account the dominant resonance. It is noted that about three terms of both series are needed to achieve an acceptable precision.

In the case of Fig. 2(c) ($k = 5k'_{11}$), the frequency exceeds the resonant frequencies of thirty-nine modes and it is close to the frequency of the TM_{72} mode. For this reason, the largest term in the one-index series is the seventh, whereas the largest term in the double series is the thirty-ninth. The series converge rapidly after the seventh or the thirty-ninth terms, respectively. It is noted that, when k increases, the number of significant terms increases more rapidly in the double series than in the one-index series.

Numerical tests carried out for different positions of the observation and the source points showed that converging properties are not affected significantly by changes in these positions. Similar results have been found for the other components of $\overline{\overline{G}}_e$.

In order to ascertain the utility of extracting the weakly singular dyadic $\overline{\overline{G}}_s$ from $\overline{\overline{G}}_e$, besides the strongly singular dyadic $\overline{\overline{G}}_i$, converging properties of our expressions have been compared with those of different expressions deriving from a representation of $\overline{\overline{G}}_e$ of the type

$$\overline{\overline{G}}_e = -\frac{1}{k^2}\nabla\nabla'\left(\frac{1}{4\pi R} + g_0\right) + \overline{\overline{G}}_\sigma \tag{31}$$

where $\overline{\overline{G}}_\sigma$ (i.e., the solenoidal part of $\overline{\overline{G}}_e$, formerly split into $\overline{\overline{G}}_s$ and $\overline{\overline{G}}'_s$) is expressed by a modal series, obtained by introducing (6), (12), and (10) or (11) into the formula

$$\overline{\overline{G}}_\sigma = \overline{\overline{G}}_e - \frac{1}{k^2}\lim_{k\to 0}\left(k^2\overline{\overline{G}}_e\right).$$

Also, $\overline{\overline{G}}_\sigma$ may be obtained in the form of a one-index or of a double series, depending on the use of (10) or (11). It is pointed out that (31) has the same form considered by Howard and Seidel [9]. Figs. 3 and 4 show that the convergence of the component $G_{rr'}$ derived from (31) (diagrams a) is much slower than the convergence of the same component in the form derived from (2) (diagrams b). This is true either in the case when $\overline{\overline{G}}_\sigma$ and $\overline{\overline{G}}'_s$ are represented by the one-index series (Fig. 3) or when they are represented by the double series (Fig. 4). As said in the introduction, the slower convergence of (31) is ascribed to the inclusion of the singularity R^{-1} in the series representing $\overline{\overline{G}}_\sigma$.

APPENDIX I

The dyadic $\bar{G}_e$, referred to the fundamental unit vectors of the spherical coordinate system, has the form

$$\bar{G}_e = \boldsymbol{r}_0\boldsymbol{r}_0' G_{rr'} + \boldsymbol{r}_0\boldsymbol{\vartheta}_0' G_{r\vartheta'} + \boldsymbol{r}_0\boldsymbol{\varphi}_0' G_{r\varphi'} + \boldsymbol{\vartheta}_0\boldsymbol{r}_0' G_{\vartheta r'} + \boldsymbol{\vartheta}_0\boldsymbol{\vartheta}_0' G_{\vartheta\vartheta'} + \boldsymbol{\vartheta}_0\boldsymbol{\varphi}_0' G_{\vartheta\varphi'} + \boldsymbol{\varphi}_0\boldsymbol{r}_0' G_{\varphi r'} + \boldsymbol{\varphi}_0\boldsymbol{\vartheta}_0' G_{\varphi\vartheta'} + \boldsymbol{\varphi}_0\boldsymbol{\varphi}_0' G_{\varphi\varphi'}.$$

The nine components $G_{rr'}, \cdots, G_{\varphi\varphi'}$ may be deduced from the five components $G_{rr'}, \cdots, G_{tt}$ with respect to the unit vectors $\boldsymbol{r}_0, \boldsymbol{r}_0', \boldsymbol{s}_0, \boldsymbol{s}_0', \boldsymbol{t}_0$ defined above, by using the relationships

$$\boldsymbol{s}_0 = c\boldsymbol{\vartheta}_0 + s\boldsymbol{\varphi}_0 \quad \boldsymbol{t}_0 = -s\boldsymbol{\vartheta}_0 + c\boldsymbol{\varphi}_0$$

$$\boldsymbol{s}_0' = c'\boldsymbol{\vartheta}_0' + s'\boldsymbol{\varphi}_0' \quad \boldsymbol{t}_0 = -s'\boldsymbol{\vartheta}_0' + c'\boldsymbol{\varphi}_0'$$

where

$$c = \frac{1}{v}[\sin\vartheta\cos\vartheta' - \cos\vartheta\sin\vartheta'\cos(\varphi-\varphi')]$$

$$s = \frac{1}{v}\sin\vartheta'\sin(\varphi-\varphi')$$

$$c' = \frac{1}{v}[\sin\vartheta\cos\vartheta'\cos(\varphi-\varphi') - \cos\vartheta\sin\vartheta']$$

$$s' = \frac{1}{v}\sin\vartheta\sin(\varphi-\varphi')$$

$$v = \sqrt{1-u^2} = \sqrt{1-[\sin\vartheta\sin\vartheta'\cos(\varphi-\varphi') + \cos\vartheta\cos\vartheta']^2}.$$

It is obtained

$$G_{r\vartheta'} = c'G_{rs'} \qquad G_{r\varphi'} = s'G_{rs'}$$

$$G_{\vartheta r'} = cG_{sr'} \qquad G_{\vartheta\vartheta'} = cc'G_{ss'} + ss'G_{tt} \qquad G_{\vartheta\varphi'} = cs'G_{ss'} - sc'G_{tt}$$

$$G_{\varphi r'} = sG_{sr'} \qquad G_{\varphi\vartheta'} = sc'G_{ss'} - cs'G_{tt} \qquad G_{\varphi\varphi'} = ss'G_{ss'} + cc'G_{tt}.$$

APPENDIX II

On application of the differential operators (26) to (18), we obtain

$$G^0_{rr'} = \frac{1}{4\pi a}\sum_1^\infty{}_n \left[\frac{2n^3+3n^2-5n-3}{(2n-1)(n+1)} - n\frac{r^2+r'^2}{2a^2}\right]\frac{nP_n(u)h^{n-1}}{2n+3}$$

$$G^0_{rs'} = \frac{v}{4\pi a}\sum_1^\infty{}_n \left[\frac{2n^3+3n^2-5n}{(2n-1)(n+1)} - \frac{nr^2}{2a^2} - \frac{n(n+3)r'^2}{2(n+1)a^2}\right]\frac{P_n'(u)h^{n-1}}{2n+3}$$

$$G^0_{ss'} = \frac{1}{4\pi a}\sum_1^\infty{}_n \left[-\frac{(2n^3+3n^2-5n-3)u}{(2n+3)(2n-1)n} + \frac{(n+3)(r^2+r'^2)u}{(2n+3)2a^2} - \frac{h}{n}\right]\frac{P_n'(u)h^{n-1}}{n+1} + \frac{1}{4\pi a}\sum_1^\infty{}_n \left[\frac{2n^3+3n^2-5n-3}{2n-1} - n(n+3)\frac{r^2+r'^2}{2a^2}\right]\frac{P_n(u)h^{n-1}}{2n+3}$$

$$G^0_{tt} = \frac{1}{4\pi a}\sum_1^\infty{}_n \left[\frac{2n^3+3n^2-5n-3}{n(2n+3)(2n-1)} - \frac{(n+3)(r^2+r'^2)}{(2n+3)2a^2} + \frac{uh}{n}\right]\frac{P_n'(u)h^{n-1}}{n+1} - \frac{1}{4\pi a}\sum_1^\infty{}_n P_n(u)h^n.$$

Making use of the recurrence formulas for Legendre polynomials, these series may be cast into the form of (28), where

$$f_1 = \frac{1}{4}\sum_1^\infty{}_n \frac{nP_n(u)h^{n-1}}{2n+3}$$

$$f_2 = -\sum_1^\infty{}_n \frac{nP_n(u)h^{n-1}}{n+1}$$

$$f_3 = -\frac{3}{2}\sum_1^\infty{}_n \frac{P_n'(u)h^{n-1}}{2n+3}$$

$$f_4 = \sum_1^\infty{}_n \frac{P_n'(u)h^{n-1}}{n+1}.$$

These series may be summed by relating them to the well-known generating function for the Legendre polynomials

$$\sum_0^\infty{}_n P_n(u)h^n = (1+h^2-2hu)^{-1/2} = f_0$$

obtaining (29). As an example

$$f_4 = \sum_1^\infty{}_n \frac{P_n'(u)h^{n-1}}{n+1} = \frac{\partial}{\partial u}\left[\sum_0^\infty{}_n P_n(u)\frac{1}{h^2}\int_0^h x^n\,dx - \frac{P_0(u)}{h}\right]$$

$$= \frac{1}{h^2}\frac{\partial}{\partial u}\int_0^h\left[\sum_0^\infty{}_n P_n(u)x^n\right]dx = \frac{1}{h^2}\frac{\partial}{\partial u}\int_0^h \frac{dx}{\sqrt{1+x^2-2xu}}$$

$$= \frac{1}{h^2}\frac{\partial}{\partial u}\ln\frac{\sqrt{1-2hu+h^2}+h-u}{1-u}.$$

For very small values of h, functions f_1, f_2, f_3, and f_4 can be approximated by the first two terms of the corresponding defining series; furthermore, for values of u close to ± 1 ($v \approx 0$), functions f_3 and f_4 may be evaluated using the following formulas:

for $u \approx +1$

$$f_3 \approx \frac{3}{8h^2(1+h)(1+u)}\left\{\left[\frac{3-2h-5h^2}{(1-h)^2} - \frac{3}{2\sin\beta}\ln\frac{1+\sin\beta}{1-\sin\beta}\right] + \left[\frac{55h^4+24h^3+2h^2+24h-9}{(1-h)^4} + \frac{9}{2\sin\beta}\ln\frac{1+\sin\beta}{1-\sin\beta}\right]\frac{1-u}{16}\right\}$$

$$f_4 \approx \frac{1}{(1+u)(1-h)^2}\left[1 - \frac{1+2h}{2(1-h)^2}(1-u)\right]$$

for $u \approx -1$

$$f_3 \approx \frac{3}{8h^2(1+h)(1-u)}\left\{\left[\frac{3+5h}{1+h} - \frac{3\beta}{\sin\beta}\right] - \left[\frac{55h^3+31h^2+33h+9}{(1+h)^3} + \frac{9\beta}{\sin\beta}\right]\frac{1+u}{16}\right\}$$

$$f_4 \approx \frac{1}{(1-u)(1+h)^2}\left[1 - \frac{1-2h}{2(1+h)^2}(1+u)\right].$$

REFERENCES

[1] A. D Yaghjian, "Electric dyadic Green's functions in the source region," *Proc. IEEE*, vol. 68, pp. 248–263, Feb. 1980.

[2] S. W. Lee, J. Boersma, C. L. Law, and G. A. Deschamps, "Singularity in Green's function and its numerical evaluation," *IEEE Trans. Antennas Propagat.*, vol. AP-28, no. 3, pp 311–317, May 1980.

[3] C. T. Tai, *Dyadic Green's Functions in Electromagnetic Theory*. Scranton, PA: Intext, 1971.
[4] L. B. Felsen and N. Marcuvitz, *Radiation and Scattering of Waves* Englewood Cliffs, NJ: Prentice Hall, 1973
[5] Y. Rahmat-Samii, "On the question of computation of the dyadic Green's function at the source region in waveguides and cavities," *IEEE Trans. Microwave Theory Tech.*, vol. MTT-23, pp. 762–765, Sept. 1975.
[6] C. T. Tai and P. Rozenfeld, "Different representations of dyadic Green's functions for a rectangular cavity," *IEEE Trans. Microwave Theory Tech.*, vol. MTT-24, pp. 597–601, Sept. 1976.
[7] M. Kisliuk, "The dyadic Green's functions for cylindrical waveguides and cavities," *IEEE Trans. Microwave Theory Tech.*, vol. MTT-28, pp. 894–898, Aug. 1980.
[8] C. T. Tai, "Dyadic Green's functions for a coaxial line," *IEEE Trans. Antennas Propagat.*, vol. AP-31, no. 2, pp. 355–358, Mar. 1983.
[9] A. Q. Howard and D. B. Seidel, "Singularity extraction in kernel functions in closed region problems," *Radio Sci.*, vol. 13, no. 3, pp. 425–429, May–June 1978.
[10] V. Daniele and M. Orefice, "Dyadic green's functions in bounded media," *IEEE Trans. Antennas Propagat.*, vol. AP-32, pp. 193–196, Feb. 1984.
[11] V. Daniele, "New expressions of dyadic Green's functions in uniform waveguides with perfectly conducting walls," *IEEE Trans. Antennas Propagat.*, vol. AP-30, pp. 497–499, May 1982.
[12] M. Bressan and G. Conciauro, "Rapidly converging expressions for dyadic Green's functions in two-dimensional resonators of circular and rectangular cross-section," *Alta Frequenza*, vol. LII, no. 3, pp. 188–190, May–June 1983.
[13] M. Bressan and G. Conciauro, "Rapidly converging expressions of electric dyadic Green's functions for resonators," in *Proc. 1983 URSI Symp. on Electromagnetic Theory* (Santiago de Compostela, Spain), Aug. 23–26, 1983, pp. 41–44.
[14] M. Bressan, G. Conciauro, and C. Zuffada, "Waveguide modes via an integral equation leading to a real matrix eigenvalue problem," *IEEE Trans. Microwave Theory, Tech.*, pp. 1495–1504, Nov. 1984.

Characteristic Impedance Design Considerations for a High-Speed Superconducting Packaging System

JIRO TEMMYO AND HARUO YOSHIKIYO

Abstract—**The characteristic impedance influences of superconducting packaging systems (in particular, Josephson packaging) on the degradation in transmitted signal rise time, amplitude distortions and crosstalk, signal propagation delay, and amplitude decay at the inductive and resistive connectors with matched capacitors are quantitatively evaluated by using the ASTAP computer simulation. The present choice of the characteristic impedance $Z_0 = 10$–$12\ \Omega$ for a superconducting stripline is inadequate. Higher impedances of $Z_0 = 40$–$50\ \Omega$ are useful from the standpoint of noise performance improvement. At the same time, a higher impedance choice can make the ground connector numbers of each connector decrease, which is preferable for a large-scale packaging system.**

I. Introduction

In order to realize high-performance computing systems utilizing high-speed devices, such as Josephson junction devices and other high-speed semiconductor devices, it is necessary to use high-density packaging systems with small wiring delays. The electrical problems in the packaging system are decreasing the noise signals such as crosstalk and reflection at the various connectors, and minimizing the packaging delay. A three-dimensional superconducting packaging system consisting of superconducting striplines [1] and small connectors is useful for high-density packaging because lossless superconducting lines have few heating problems [2].

A matched-signal propagation system with superconducting striplines has excellent features such as a broad transmission frequency band and almost lossless characteristics. Conversely, signal distortion problems occur compared with other lossy packaging systems because the reflected signals and crosstalk do not decrease [3]–[6]. Added delays due to a matched capacitor at the inductive connectors, crosstalk between signal lines, and signal decay at the resistive connectors decrease the system operating margin.

On the other hand, electrical design considerations of a high-speed semiconductor computer package have been carried out by E. E. Davidson from the standpoint of system noise tolerance performance [7]. However, noise performance of the superconducting packaging system from the standpoint of the characteristic impedance influences on the system has not been determined.

The purpose of this paper is to clarify the optimum characteristic impedance design method for superconducting packaging systems, particularly the Josephson packaging system. The characteristic impedance influences of superconducting packaging systems on the noise performance, such as reflection and crosstalk etc., which are caused by the inductive connectors, was clarified by using the ASTAP [8] computer simulation. From the relationships between the characteristic impedance Z_0 and noise, delay performances are clarified as design charts. It is proposed that present choices of $Z_0 = 10$–$12\ \Omega$ are not adequate and higher values of Z_0 are superior from the standpoint of low noise and small delay performances of the system using a high-output superconducting driver and highly sensitive receiver circuits.

II. Circuit Simulation

A schematic and electrical diagram of the chip-to-chip signal path is shown in Fig. 1, where L_c^C is the chip-to-card bonding [9], [10] inductance, L_c^F is the fillet [11] inductance, L_c^{MC} is the microconnector [12] inductance, and R_c^C, R_c^F, and R_c^{MC} are the interconnection resistance at the chip bonding, fillet, and microconnector, respectively. Except for the mutual inductance of M_c^C at the chip bonding, other connector mutual inductances of M_c^F and M_c^{MC} are omitted for simplicity. Z_0 is the superconducting transmission-line impedance of the chip and the package. In a small Josephson system experiment [13], the rise time of the driver's output signal was increased to about 100 ps by an LC filter to reduce crosstalk and minimize the reflections from the inductive discontinuities of the microconnectors. Here, in order to reduce absolute values of self- and mutual-inductances, the ratio of signal connectors to ground connectors was 1 for both pins and fillets. However, the increase of that ratio is important and necessary, particularly when the packaging system becomes larger.

The signal reflection and crosstalk at the inductive connectors are determined by the absolute value of the inductances and the characteristic impedance Z_0, as shown in Fig. 2. Time-domain responses for the circuit of Fig. 1 are shown for the cases of $Z_0 = 10\ \Omega$ and $20\ \Omega$, using the ASTAP computer simulation. The current traces of Nos. 1–6 show the current waveforms at the portion Nos. 1–6 in Fig. 1 and the degradation of the transmitted high-speed signal. Here, it is assumed that the Josephson driver is approximated as a ramped input voltage positive going source. The entire lossless superconducting stripline length at chips, cards, fillets, and cards is a constant 4 mm, i.e., the propagation

Manuscript received July 27, 1984; revised January 4, 1985.
The authors are with Atsugi Electrical Communication Laboratory, Nippon Telegraph and Telephone Public Corporation, 1839 Ono, Atsugi-shi, Kanagawa 243-01, Japan.

0018-9480/85/0500-0414$01.00 ©1985 IEEE